Journal of Catalysis **186,** 353–361 (1999)
Article ID jcat.1999.2566, available online at http://www.idealibrary.com on IDEAL®

A Transient Kinetic Study of the Mechanism of the $NO + H_2$ Reaction over Pt/SiO_2 Catalysts

1. Isotopic Transient Kinetics and Temperature Programmed Analysis

R. Burch, A. A. Shestov,[1] and J. A. Sullivan

Catalysis Research Centre, Department of Chemistry, The University of Reading, Whiteknights, Reading, RG6 6AD, United Kingdom

Received February 4, 1999; revised May 11, 1999; accepted May 11, 1999

The $NO + H_2$ reaction has been studied over a supported Pt catalyst using temperature programmed reaction (TPR_{xn}), temperature programmed desorption (TPD), and steady state and non-steady state isotopic transient kinetic analysis (SSITKA and NSSITKA). N_2, N_2O, and NH_3 formation are noted during the TPR_{xn}. N_2O is the most prevalent species formed at lower temperatures while N_2 is most prevalent at higher temperatures. NH_3 is formed in relatively low yields at intermediate temperatures. The SSITKA shows that N_2O is the isotopically first product and that N_2 is isotopically second. The concentration of sites producing N_2O and N_2 increases with temperature, and the increase in the effective activity of the sites is greater for those sites producing N_2 than those sites producing N_2O. The chemisorption of NO is also found to be a reversible process under actual reaction conditions. Non-steady state transient kinetic experiments show that after removal of the gas phase NO, there is a conversion of some of the residual NO on the surface into N_2 precursors following a short treatment in a H_2 whereas N_2O precursors on the surface are destroyed by this treatment. It is concluded that the formation of N_2O requires the presence of gas-phase or very weakly adsorbed NO.

Key Words: **Pt catalysts; NO reduction; reaction mechanism; TPD; TPR_{xn}; SSITKA.**

INTRODUCTION

The removal of nitrogen oxides (NOx defined as $NO + NO_2$) from exhaust streams of stationary and mobile power sources has been a topic of much discussion in the literature for the past 25 years (1–6) and the detrimental effects of NOx on the environment and to personal health are well known (7, 8). Therefore the removal of NO from the exhausts of combustion sources remains a challenging scientific and technical problem. No NO decomposition catalyst is yet active enough at the temperatures of interest to be an efficient deNOx agent (9). Current technologies for the removal of NOx rely on reducing agents either added to (e.g., in the case of the NH_3 selective catalytic reduction process (2)) or already present in the exhaust stream (in the case of a three-way catalyst NOx reduction (1)).

The removal of NOx under net oxidising conditions is still a problem for mobile power sources, e.g., lean-burn gasoline and diesel engines (10). Many catalyst formulations and hydrocarbon reductants have been tested in the NO/hydrocarbon/O_2 reaction (11–13), but supported Pt catalysts remain among the most promising (14–17).

H_2 is a potential reductant for NO since the internal combustion engine can be tuned to produce significant amounts of H_2 from gasoline. This might be an attractive solution to the NO emission problem under cold start conditions and for some specific diesel applications where the exhaust temperature is low. Supported Pt catalysts are active for the production of N_2 and N_2O from the $NO + H_2$ reaction both in the presence and in the absence of O_2 (18). However, the production of N_2O also creates environmental problems (19).

Steady state isotope transient kinetic analysis (SSITKA), developed by Happel (20), Bennett (21), and Biloen (22), has previously been used to clarify the mechanisms of several reactions, e.g., Fischer–Tropsch synthesis (23), CO hydrogenation (24), oxidative coupling of CH_4 (25), and methanol synthesis (26). As a general rule the reactions which provide the clearest information are those in which the surface contains large reservoirs of adsorbed intermediates which are slowly transformed to products.

SSITKA of the CO oxidation and CO/NO reactions over three-way catalysts (27) and aged Pt–Rh catalysts (28) have been published. Efstathiou *et al.* (29) and Janssen *et al.* (30) have studied the $NO/NH_3/O_2$ reaction over V_2O_5/TiO_2 catalysts. Ozkan *et al.* (31) have studied the $NO/CH_4/O_2$ reaction over Pd/TiO_2 catalysts. We have recently completed an analysis of the $NO/C_3H_6/O_2$ reaction over Pt/SiO_2 catalysts (32, 33).

In the present work, the $NO + H_2$ reaction is studied over a supported Pt catalyst (5% Pt/SiO_2) using temperature programmed reaction/desorption and isotopic transient

[1] On leave from Boreskov Institute of Catalysis, Russian Academy of Sciences, Pr. Akademika Lavrentieva, 5, Novosibirsk, 630090, Russia.

0021-9517/99 $30.00

kinetic analysis (both steady state and non-steady state) in an attempt to understand more about the nature of the surface intermediates in the formation of N_2 and N_2O.

EXPERIMENTAL

One hundred and thirteen milligrams of a sample of 5% Pt/SiO_2 with a metal dispersion of 31% was placed in a tubular quartz reactor. The catalyst was preceded by 100 mg of quartz chips which serve to preheat the incoming gas. The reactor was configured to minimise the dead volume in front of the catalyst. The sample was pretreated in an H_2 stream at 450°C prior to any measurements being taken.

For the *temperature programmed reaction* experiment the catalyst was held in the reaction mixture at 300°C for 1 h and cooled in the mixture to room temperature. The reaction mixture contained 1.8% NO (from a cylinder of 5% Ar in NO) and 1.8% H_2 (from a cylinder of 3% H_2 in He), and it was balanced using He to give a total flow of 103 cm^3 min^{-1}. Gas flow rates were controlled using Bronkhurst mass flow controllers. The temperature was ramped at 5°C min^{-1} to 350°C and NO, NH_3, N_2, N_2O, and H_2O were monitored as a function of temperature.

The percentage conversions of reactant from NO into NH_3, N_2, and N_2O were calculated from observed mass spectrometer partial pressures and calibration plots of ppm versus partial pressure.

Temperature programmed desorption (TPD) experiments were carried out on a prereduced Pt/SiO_2 catalyst. One hundred and thirteen milligrams of catalyst was pretreated in the reducing gas (10% H_2 in He, 100 cm^3 min^{-1}) at 500°C for 1 h, cooled to room temperature, dosed in NO (2% NO in He 100 cm^3 min^{-1}) for 1 h, and purged in He at the same temperature, again for 1 h. The temperature was then ramped (20°C min^{-1}) while the catalyst was held in an He flow (100 cm^3 min^{-1}) and the effluent monitored by a mass spectrometer. Concentrations of NO, NO_2, N_2O, NH_3, and N_2 were continuously analysed as a function of temperature.

For the *steady state isotopic transient kinetic analysis* studies the catalyst was held in the reaction mixture at 300°C for 1 h, cooled to room temperature, and then heated (at 5°C min^{-1}) to the reaction temperature. The sample was held at the reaction temperature until steady state reaction conditions were attained (usually 20 min was sufficient although longer times were needed around the temperature of H_2 "light-off").

The NO/Ar mixture in the stream was then removed and replaced with a flow of ^{15}NO (at the same flow rate and pressure). This switch was carried out when the catalyst was operating at steady state. Therefore, information about the surface of the catalyst *under steady state conditions* can be determined from the measured profiles of the reactant and product molecules. The pressures of the in-switched and out-switched NO can be different due to the back-pressure caused by the presence of the catalyst in the line containing the unlabelled NO/Ar mixture. To overcome this problem the pressure between these two gas lines was equalised by creating a back-pressure in the labelled line using a fine needle valve at the outlet. The pressure created in both lines, and the difference in pressure between the lines, was monitored using two "Wika" pressure transducers.

Once the ^{14}NO/Ar mixture was removed, the decay in ^{14}N-containing products (NH_3, N_2, N_2O) could be monitored by a mass spectrometer (Gaslab 300) which was connected to the exhaust of the reactor by a continuously evacuated heated capillary. The formation and decay of mixed labelled products ($^{14}N^{15}N$ and $^{14}N^{15}NO$), as well as the formation of doubly labelled species ($^{15}N_2O$), could also be followed. The formation of $^{15}N_2$ cannot be followed as the mass of this species overlaps with that of ^{14}NO. $^{14}NH_3$ and $^{15}NH_3$ can be discerned after the contributions of various water fragments to their respective signals have been factored out (34). This is made more straightforward by virtue of the fact that the H_2O signal is a constant before and after the switch. The decrease in the ^{14}NO and the corresponding increase in the ^{15}NO following the switch can also be followed and this gives information about the reversibility of the reactant adsorption. All the generated profiles can be compared with the Ar profile which itself is indicative of the gas-phase holdup of the system. The lag time for the Ar signal was approximately 1.5 s.

Further *non-steady state transient kinetic analysis* was also carried out. This involved ^{15}NO switching experiments where the catalyst was not maintained at steady state. In these reactions the catalyst was brought to steady state in the $^{14}NO/H_2$ mixture and the ^{14}NO was removed from the stream and replaced with Ar/He at the same flow rate. The catalyst was then held in the H_2/Ar mixture for a definite time and then the Ar was replaced with ^{15}NO. All product and reactant signals were followed after this switch, but the ones of interest are those of the mixed labelled $^{14}N^{15}N$ and $^{14}N^{15}NO$ (or $^{15}N^{14}NO$) profiles. What we are attempting to measure in these experiments is the titration of the remaining ^{14}N species from the surface by the switching-in of the ^{15}NO.

RESULTS

Temperature Programmed Reaction

Figure 1 shows the temperature programmed reaction profiles seen for the $NO + H_2$ reaction over the 5% Pt/SiO_2 catalyst. The profile for NH_3 is deduced from the $m/e = 17$ profile after taking into account the contribution for H_2O at $m/e = 18$. It can be seen that the NO conversion profile goes through a maximum at ca. 100°C and then rises to almost 100% at 210°C. Three products are noted. N_2O is first seen

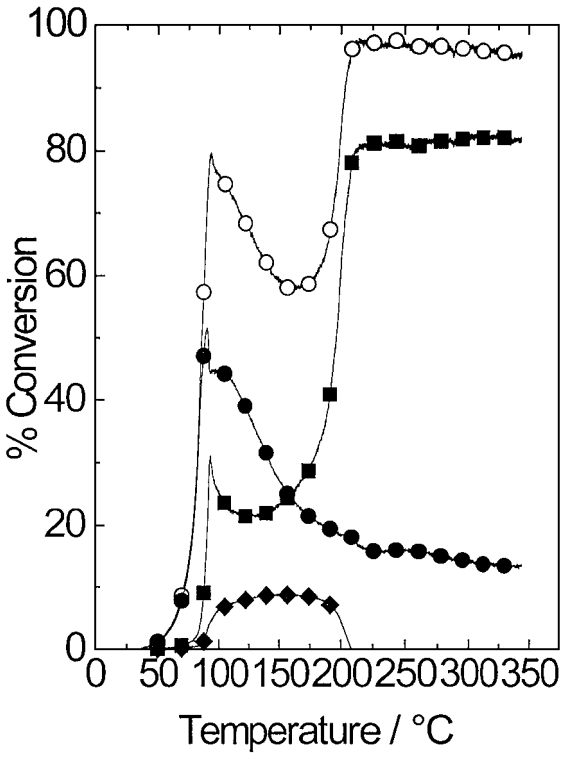

FIG. 1. Temperature programmed reaction between NO and H_2 over 5% Pt/SiO_2. Reaction conditions: 1.8% NO, 1.8% H_2, total flow 103 cm^3 min^{-1}, catalyst mass 113 mg, ramp rate 5°C min^{-1}. Conversion to N_2 (■), N_2O (●), and NH_3 (◆), and conversion of NO (○).

at 50°C. N_2 is observed at 70°C, and NH_3 at 90°C. The production of N_2O goes through a maximum at a temperature of ∼90°C and then decreases smoothly. N_2 production goes through a maximum at a slightly higher temperature. The amount of N_2 then decreases to a minimum at ∼125°C, before increasing to reach a plateau at 210°C. Conversion to NH_3 is first observed when the conversion to N_2O reaches its maximum, and the amount of NH_3 remains steady until a temperature of ∼180°C, at which point it quickly decreases to zero.

Steady State Isotopic Transient Kinetic Analysis

Three temperatures (50, 60, and 73°C) were chosen for SSITKA under differential conditions. Conversion to N_2O was far more prevalent than conversion to N_2, and there was no discernible conversion to NH_3. For comparison, experiments were also carried out at 125 and 185°C, where the conversion of NO is very high and therefore the reactor was operating under nondifferential conditions but this did allow us to investigate the formation of NH_3. Values for the rates of production of N_2, N_2O, and NH_3, as well as the flow rate of unreacted NO, are presented in Table 1.

Figure 2 shows a typical product profile obtained after the switch from ^{14}NO to ^{15}NO at 60°C. The unlabelled products ($^{14}N_2$ and $^{14}N_2O$) are found to decrease from normalised values of 1 to zero after the switch. Simultaneously, the mixed labelled species ($^{14}N^{15}N$, $^{14}N^{15}NO$, and $^{15}N^{14}NO$) are seen to rise to a maximum, and then return to the background level, while the doubly labelled species ($^{15}N_2$ and $^{15}N_2O$) rise from values of zero to their normalised values of 1.

Figure 3 shows the analysis of these experimental results in terms of α, where α represents the fraction of heavy atoms in the gas phase in a particular molecule. For example, $\alpha(N_2)$ is defined as

$$\alpha(N_2) = \frac{[^{15}N_2] + 0.5[^{15}N\,^{14}N]}{[^{15}N_2] + [^{14}N\,^{15}N] + [^{14}N_2]}. \qquad [1]$$

It can be seen that the α profiles for N_2O and for NO coincide, while the profile for N_2 rises much more slowly. The fact that the profiles for α(NO) and $\alpha(N_2O)$ are the same indicates that N_2O molecules which contain a 14-labelled N atom can only continue to be formed from ^{14}NO while ^{14}NO remains in contact with the catalyst. This shows that an Eley–Rideal-type mechanism might operate here. The presence of a relatively large reservoir of N_2O forming intermediates is indicated by the difference between the $\alpha(N_2O)$ profile and that of the Ar. The difference between

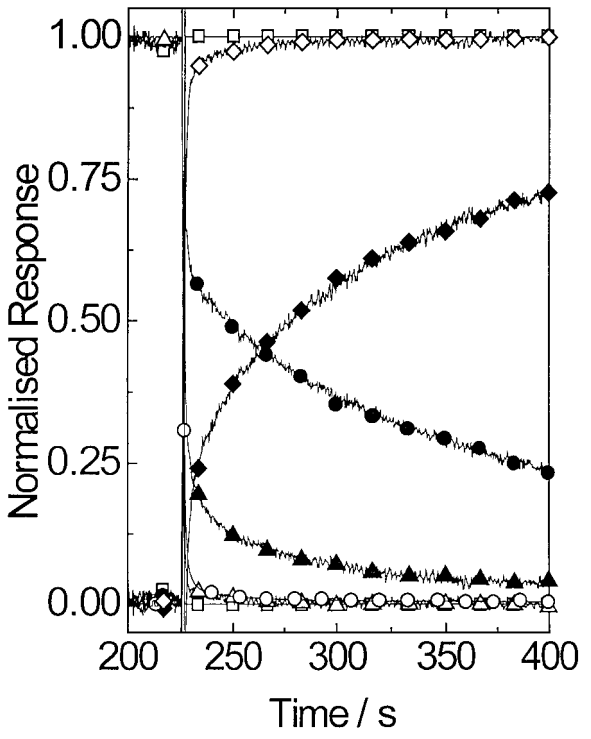

FIG. 2. Normalised product responses following the replacement of ^{14}NO/Ar with ^{15}NO in the reaction stream. Reaction conditions: 1.8% NO and H_2, total flow 103 cm^3 min^{-1}, catalyst mass 113 mg, $T = 60$°C. $^{14}N_2$ (▲), $^{14}N^{15}N$ (●), $^{15}N_2$ (◆), $^{14}N_2O$ (△), $^{14}N^{15}NO$ (or $^{15}N^{14}NO$) (○), $^{15}N_2O$ (◇), Ar and inverse Ar (□).

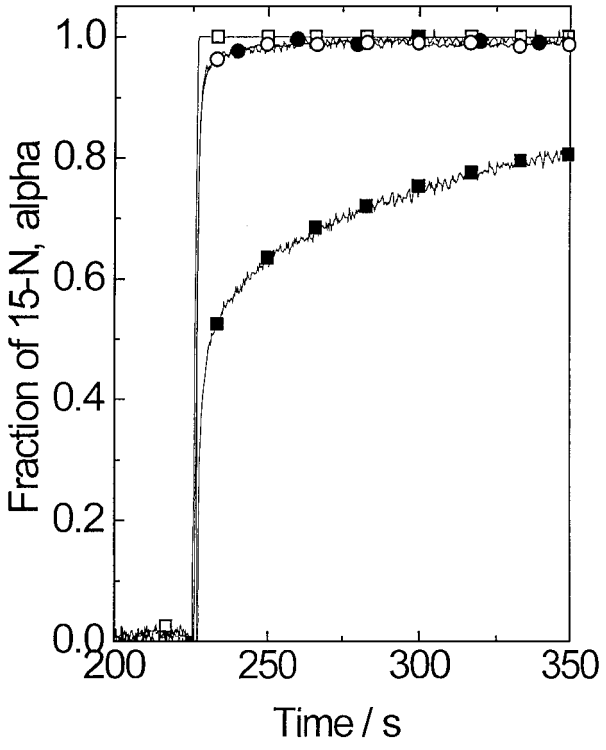

FIG. 3. Profile of the α functions following the replacement of ^{14}NO/Ar with ^{15}NO in the reaction stream. Reaction conditions: 1.8% NO and H_2, total flow 103 cm^3 min^{-1}, catalyst mass 113 mg, $T = 60^\circ$C. αN_2 (■), αN_2O (●), αNO (○), and inverted Ar (□) profile.

the α(NO) profile and the Ar profile indicates a steady state desorption of NO from the catalyst under working conditions.

Figure 4 shows a similar plot in which the experiment was carried out at 125°C, where NH_3 is formed. It must be remembered that under these conditions the reactor is not behaving differentially as the conversion of NO is ~86%. In this profile it is seen that the N_2O is still "isotopically first" and N_2 is "isotopically second." The α(NO) profile lags behind the N_2O and N_2 profiles, a situation that is unusual in SSITKA but which can be explained in terms of a nondifferential reactor. Such a large delay in the α(NO) profile, i.e., a situation where $\tau(NO) \gg \tau(N_2)$, $\tau(N_2O)$, has been seen previously in SSITKA of the $NO/C_3H_6/O_2$ reaction over similar Pt/SiO_2 catalysts when the catalyst was operating under nondifferential conditions (conversion of $C_3H_6 = 100\%$) (33). In that case the delay was ascribed to the change between a reduced surface (presumably at the beginning of the catalyst bed) where N_2 and N_2O formation takes place and an oxidised Pt surface (presumably lower down the catalyst bed) where no N_2 or N_2O formation takes place.

On the oxidised Pt surface the NO can adsorb more strongly (as NO_2 or ONO-type species), and thus it takes longer for the ^{14}NO molecules to be removed from the reactor. N_2 and N_2O product molecules do not interact in this manner with this oxidised portion of the catalyst and thus the α(NO) profile is delayed longer than the $\alpha(N_2)$ and $\alpha(N_2O)$ profiles.

The $\alpha(NH_3)$ profile is further delayed again relative to the α(NO), which is consistent with NH_3 being the isotopically third product, although, as with NO, a slow release of NH_3 would give the same profile.

These normalised plots can be analysed to provide values for τ (the mean surface residence time for intermediates leading to products). This is calculated from the difference in area under plots of α and the inert tracer (Ar). For example, in the case of N_2,

$$\tau_{(N_2)} = \int_0^\infty \tilde{\alpha}(N_2)\, dt, \qquad [2]$$

where $\tilde{\alpha}$ represents the $(1-\alpha)$ profile in the case of the ^{14}NO to ^{15}NO switch and the α profile in the case of the ^{15}NO to ^{14}NO switch. The "mean surface lifetime" of the species leading to product as well as the rates of formation of the various products are also shown, as a function of temperature, in Table 1. These values can be used in conjunction with each other to yield values for the average concentration of adsorbed surface species leading to product and of adsorbed reactant which simply desorbs. For example, in

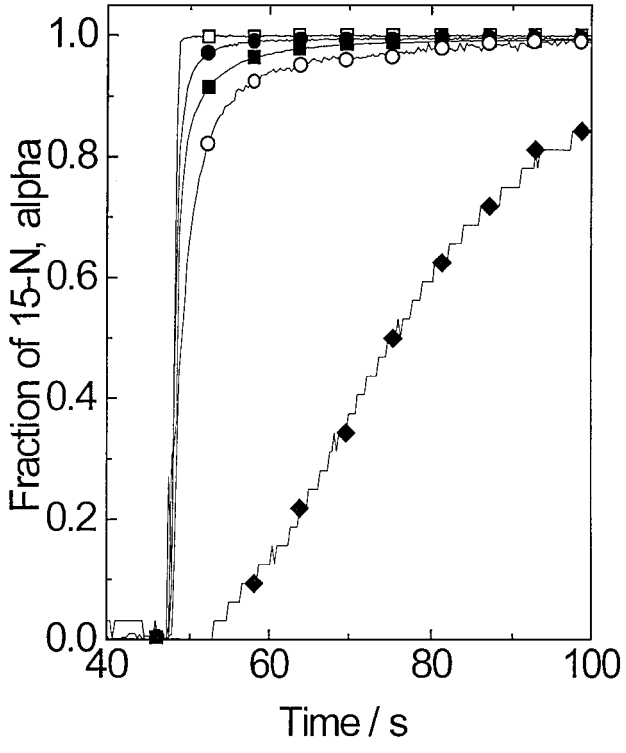

FIG. 4. Profile of the α functions following the replacement of ^{14}NO/Ar with ^{15}NO in the reaction stream. Reaction conditions: 1.8% NO and H_2, total flow 103 cm^3 min^{-1}, catalyst mass 113 mg, $T = 125^\circ$C. αN_2 (■), αN_2O (■), αNO (○), αNH_3 (◆), and inverted Ar (□).

TABLE 1

Rates of Formation of N_2, N_2O, and NH_3 and the Flow Rate of Unreacted NO (μmol g^{-1} s^{-1}) over a 5% Pt/SiO_2 Catalyst at Various Temperatures in an NO + H_2 Stream

T(°C)	$r(N_2)$	$\tau(N_2)$	$r(N_2O)$	$\tau(N_2O)$	$r(NH_3)$	$\tau(NH_3)$	r(NO)	τ(NO)
50	0.04	37	0.25	1.7	—	—	10.6	1.7
60	0.09	34	0.59	1.3	—	—	9.8	1.3
73	0.3	22	1.6	1.2	—	—	7.0	1.4
125	1.6	1.6	2.9	0.7	0.62	35	1.5	3.3
185	1.9	1.7	1.4	0.8	0.83	19	3.8	8.1

Note. Values for τ (the mean surface residence time (s)) for the products and reactant as determined from SSITKA are also given. The reactant stream contained 1.8% NO, 1.8% H_2, balanced with He to 103 cm^3 min^{-1} over 113 mg catalyst.

the case of N_2 or N_2O this is calculated from the relationship (35)

$$2 * \tau_{(\text{total})} * r_{(N_2 \text{ or } N_2O)} = N_{(N_2 \text{ or } N_2O)}, \quad [3]$$

where τ is the mean surface residence time (s), r is the rate of production of the product molecules (μmol g^{-1} s^{-1}), and N is the concentration of surface intermediates leading to the corresponding products (μmol atoms g^{-1}). The number 2 represents the number of atoms of labelled element per molecule (2 in the case of N_2 and N_2O, 1 in the case of NO and NH_3).

In our case, for the switch $^{14}NO + H_2 \rightarrow {}^{15}NO + H_2$, where the products of the reaction are N_2, N_2O, and NH_3, we can calculate the total concentration of N-labelled surface intermediates from the equation

$$q \cdot \left(C_{NO}^{out}\right) \int_0^\infty (1-\alpha_{NO})\,dt + 2 \cdot q \cdot C_{N_2}^{out} \int_0^\infty (1-\alpha_{N_2})\,dt + 2 \cdot q \cdot C_{N_2O}^{out} \int_0^\infty (1-\alpha_{N_2O})\,dt + q \cdot C_{NH_3}^{out} \int_0^\infty (1-\alpha_{NH_3})\,dt = m_{cat} \cdot N_{Tot}, \quad [4]$$

where C refers to the outlet concentration of labelled reactants or products (mol dm^{-3}), q represents the total flow rate (dm^3 s^{-1}), m represents the catalyst mass, and N represents the average total concentration of all surface intermediates. A more general expression for the calculation of the concentration of surface intermediates from the α profiles for an arbitrary reaction has been presented previously (33).

Table 2 shows the average "individual" and total concentration of surface sites as determined following such analysis. At the lower temperatures (50 or 60°C) the qualitative "reactivity" of the sites producing N_2, as estimated from the reciprocal of the τ value (see Table 1), does not increase dramatically as the temperature is raised. It must be remembered that the reactivity—as so estimated—is only a rough measure. The $k = 1/\tau$ relationship only truly holds for a first-order unidirectional step. However, for comparing the activity of sites producing N_2 (or N_2O) at different temperatures, it is a useful guide. It is not useful for comparing the "activity" of sites producing N_2 with those producing N_2O.

Thus, the reason for the increased rate of production of N_2 is the increased concentration of sites which form N_2 (going from ~3 to ~6 μmol g^{-1} (see Table 2)). On further increase in the temperature the number of sites again increases (rising to 13.6), but now the reactivity is also significantly higher (with the τ value falling from ~34 to ~22 s).

At even higher temperatures the concentration of sites for N_2 production decreases again, but the "activity" is markedly increased and thus the rates of N_2 production are greater. Note, however, that under these conditions the reactor is not differential and thus the concentrations of surface intermediates (N (μmol g^{-1})) and metal surface coverages (Θ), calculated later, simply reflect average values over the whole of the catalyst bed.

For N_2O production Table 1 shows that, within experimental error (0.5 s), there is no change in the τ values, as the temperature is raised between 50 and 73°C. Combination of Tables 1 and 2 then shows that the increase in the rate of production between 50 and 73°C is due to an increase in the concentration of the sites which are active for this reaction.

NH_3 production is only observed at the higher temperatures. However, between the two temperatures studied the concentration of sites decreases by ~30% while the "reactivity" of the sites doubles (τ goes from 35.4 to 18.8). This results in the rate of formation of NH_3 increasing from 0.62 μmol g^{-1} s^{-1} to 0.83 μmol g^{-1} s^{-1}. It must be remembered that these values reflect an average over the whole of the catalyst bed.

With respect to NO we can see that the concentration of sites from which NO desorbs without reacting under steady state conditions decreases as the temperature is raised. At the highest temperatures, both the mean surface residence

TABLE 2

Average Concentrations of Co-adsorbed Species, N (μmol atoms g^{-1}), Leading to the Corresponding Products, on the Surface of 5% Pt/SiO_2 as a Function of Temperature during the NO + H_2 Reaction as Determined by Eqs. [2] and [3]

T(°C)	$N(N_2)$	$N(N_2O)$	$N(NH_3)$	N(NO)	$\sum N$
50	3.0	0.9	0	18.0	21.9
60	6.1	1.5	0	12.7	20.3
73	13.1	3.8	0	9.8	26.7
125	5.1	4.0	21.9	5.0	36.0
185	6.5	2.2	15.6	30.8	55.1

Note. Reactant stream contained 1.8% NO, 1.8% H_2, balanced with He to 103 cm^3 min^{-1} over 113 mg catalyst.

TABLE 3

Coverages (Θ) of Surface Intermediates on 5% Pt/SiO_2 as a Function of Temperature during the NO + H_2 Reaction as Measured by SSITKA

	$100*\Theta(N_2)$	$100*\Theta(N_2O)$	$100*\Theta(NH_3)$	$100*\Theta(NO)$	$100*\Theta(Tot)$
50	3.8	1.1	0	22.9	27.8
60	7.8	1.9	0	16.1	25.8
73	16.7	4.8	0	12.5	33.9
125	6.5	5.1	27.8	6.4	45.7
185	8.3	2.8	19.8	39.1	70.0

Note. Reactant stream contained 1.8% NO, 1.8% H_2, balanced with He.

times and the concentration of sites from which unreacted NO desorbs increase dramatically. This has been mentioned above and ascribed to a change in the surface state of the Pt, i.e., between a metal and an oxygen-covered metal. NO adsorbs on the metal simply as NO_{ads} (probably through the N atom) whereas on the O-covered metal surface it can adsorb as an ONO or an NO_{2ads} species which can be bi- or tri-dentate to the surface. In this way the interaction is no longer an NO–Pt interaction but rather a stronger NO–O–Pt interaction. We can correlate this behaviour to an increase in the O_{ads} level on the catalyst.

Table 3 shows the surface coverage of Pt with species leading to N_2, N_2O, and NH_3, as well as the surface coverage of adsorbed unreacted NO as a function of temperature. At the three lower temperatures the Pt surface is never more than 35% covered with N-containing species which go on to form either N_2 or N_2O or desorb as unreacted NO. The remainder of the surface may be covered with O_{ads}, H_{ads}, OH, or N-containing species which simply act as spectators.

Non-steady State Transient Kinetic Analysis

To examine whether gaseous NO (or the weakly adsorbed NO with which it is in rapid equilibrium) has a direct influence on the production of N_2O the following non-steady state isotopic transient kinetic (NSSITKA) experiments were performed. First, the reaction was brought to steady state in NO/Ar + H_2. The ^{14}NO/Ar mixture was then replaced by an equivalent flow of Ar/He and the catalyst was left in this H_2/Ar/He stream. Finally the ^{15}NO was switched into the reactant stream after various periods of time.

Figure 5 and Table 4 show the profiles and the total amounts for the mixed N_2 (Fig. 5a) and mixed N_2O (Fig. 5b), species following five such experiments. The first profile is obtained from a "true" SSITKA switch, i.e., with no delay between the removal of the ^{14}NO and the introduction of the ^{15}NO. Subsequent profiles correspond to delays of 30, 60, 300, and 600 s between the removal of the ^{14}NO and the switching-in of the ^{15}NO. These experiments represent a titration of the "active" ^{14}N species remaining on the Pt surface.

The first point to note is that when there is an intermediate treatment in H_2, no ^{14}NO, $^{14}N_2$, or $^{14}N_2O$ is released when the sample is then contacted with ^{15}NO. Also, the total amount of ^{14}N species on the surface is greatly decreased by any treatment in H_2 (from ~20 μmol g^{-1} to ~4 μmol g^{-1} (compare Table 2 at 60°C and Table 4)). It can be seen

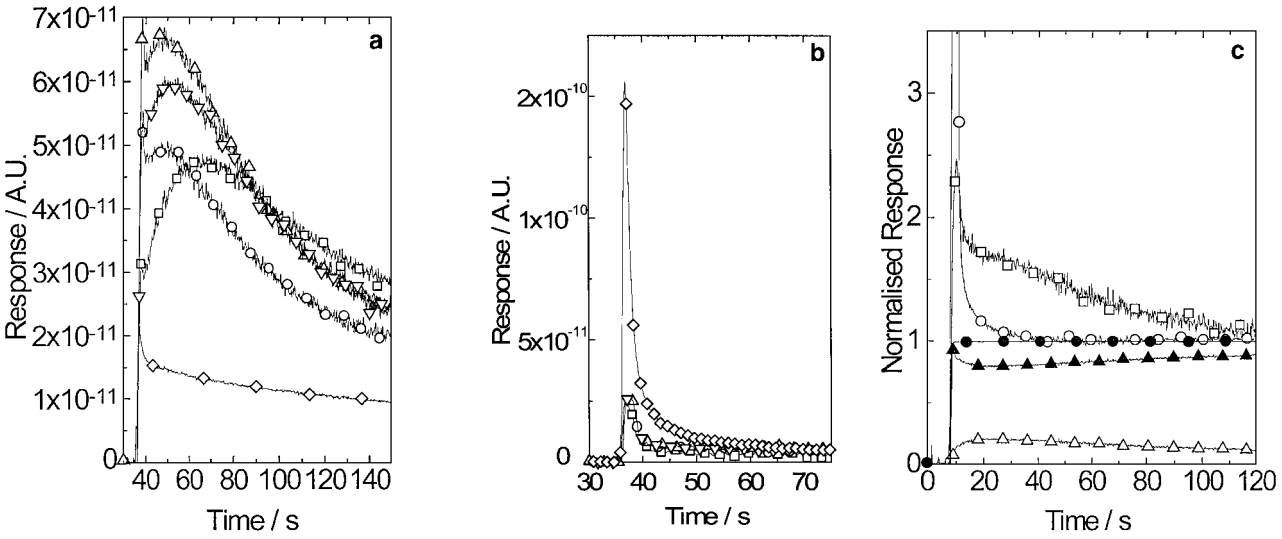

FIG. 5. Mixed labelled N_2 (a) and N_2O (b) responses following the final switch in the reaction sequence NO/Ar + H_2 → Ar + H_2 (for a variable time) → ^{15}NO + H_2 over 5% Pt/SiO_2 at 60°C. Times in the H_2/Ar stream 0 (◇), 30 (▽), 60 (△), 300 (○), and 600 s (□). Part (c) shows an example of the transient increased production of N_2 and N_2O when ^{15}NO is switched into the gas stream in place of Ar following 60 s in the H_2 stream: inverted Ar (●), normalised N_2 (□), normalised N_2O (○). Also shown are profiles describing the isotopic composition of N_2, fraction of $^{14}N^{15}N$ (△), and fraction of $^{15}N_2$ (▲).

TABLE 4

Total Production of Mixed Labelled N_2 and N_2O (μmol g^{-1}) Following the Gas Delivery Sequence $^{14}NO + H_2 \rightarrow H_2$ (t) $\rightarrow {}^{15}NO + H_2$ where the Intermediate Time (t) in the Absence of Any Gaseous NO Is Varied as Indicated ($T = 60°C$)

Time (t) in H_2 flow	Amount of N*N (μmol g^{-1})	Amount of N*NO (μmol g^{-1})
None	0.45	0.39
30 s	3.8	0.17
60 s	3.9	0.19
300 s	3.1	0.17
600 s	3.7	0.12

that the concentration of the mixed-labelled N_2O species decreases drastically once there is a time interval between the removal of the ^{14}NO and the introduction of the ^{15}NO. On the other hand, it is seen that the concentration of the mixed-labelled N_2 actually increases by about a factor of 8.

Table 4 shows that the increases in the amounts of $^{14}N^{15}N$ formed following the introduction of ^{15}NO are much greater than the decreases in the amounts of $^{14}N^{15}NO$ (or $^{15}N^{14}NO$ formed). Thus, there must be some other source of ^{14}N on the catalyst surface that becomes available for N_2 formation after the removal of gaseous NO. This indicates (a) that there are N_2-forming intermediates on the catalyst surface which are very stable at these temperatures and (b) that the presence of gaseous NO during steady state reaction causes these to form N_2O or to simply desorb.

It should also be noted that the time spent in the H_2 purge results in a more active N_2/N_2O forming catalyst. This is seen by the fact that there is a transient rise in the total N_2/N_2O profiles once the ^{15}NO is switched into the stream (Fig. 5c). There is a fast and also a relatively slow relaxation process for the N_2 transient, while the relaxation of the N_2O transient is a single fast process. Figure 5c also shows the fractional isotopic composition of the N_2 species ($^{14}N^{15}N$ (△) and $^{15}N_2$ (▲)), and this reveals that almost 100% of the N_2 formed directly following the switch was $^{15}N_2$. Shortly after the switch the fraction containing a 14-N atom becomes significant. This decreases slowly with time following the switch as the reservoir of ^{14}N species on the surface is depleted.

This transient increase associated with an increased exposure to H_2 can be explained by the removal of O_{ads} creating dissociation sites and possibly also as a result of increasing the H_{ads} coverage. This "adsorbate assisted reaction" of NO, assisted by the presence of H_{ads}, has been reported previously on Rh/SiO_2 and Pt/SiO_2 (37, 38).

Temperature Programmed Desorption

The TPD-NO profiles from the prereduced catalyst are given in Fig. 6. The absolute amounts of desorbed species

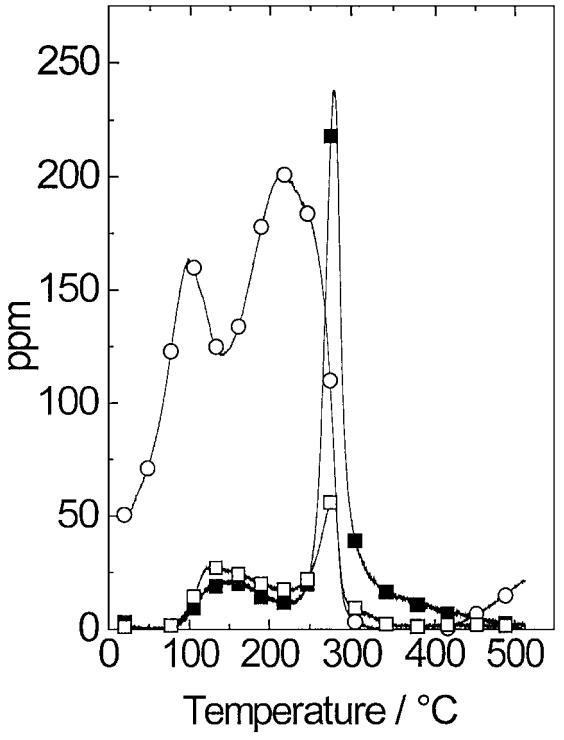

FIG. 6. Temperature programmed desorption of NO from 5% Pt/SiO_2 following a pretreatment in H_2 at 500°C, an NO dose at room temperature, and an He purge at room temperature for 1 h. Ramp rate 20°C min^{-1}, catalyst mass 113 mg, total He flow 100 cm^3 min^{-1}: N_2 (■), N_2O (□), and NO (○).

and the temperatures of the peak maxima are listed in Table 5. N_2 and N_2O formation, as well as NO desorption, were seen during the TPD. There was no desorption of NO_2 or O_2 noted. There are two desorption ranges for N_2 and N_2O formation. One is centred at around 150°C, and the second is seen as sharp peaks at 180°C.

The lower temperature formation of N_2 and N_2O can be related to the increased availability of sites as the NO desorption progresses, i.e., as NO desorbs then some NO

TABLE 5

Absolute Amounts Desorbed and Temperatures of Desorption maxima following a TPD of NO from a 5% Pt/SiO_2 which Had Been Prereduced (Fig. 6)

	T_{max} (°C)	μmol g^{-1}
N_2	144	4.0
N_2	278	15.9
NO	104	32.3
NO	225	36.9
N_2O	135	5.2
N_2O	278	5.1

Note. Ramp rate, 20°C min^{-1}; catalyst mass, 113 mg; total flow, 100 cm^3 min^{-1}.

can adsorb in a bi-dentate manner (through both the N and the O). These species might then interact with molecular NO to form N_2 and N_2O. As this concentration of molecular NO decreases (due to desorption), the production of N_2 and N_2O through this route reaches a maximum and also begins to decrease.

The higher temperature formation of N_2 and N_2O might then be caused by a second mechanism. At these temperatures NO can dissociate on the surface, without the interaction of a second molecule of NO, forming N_{ads} and O_{ads} species. The combination of the N_{ads} species with each other, or with another molecular NO species, could generate the N_2 and N_2O products, respectively. This leads to the sharp production of N_2 and N_2O centred at 280°C.

This also explans the shape of the NO desorption profile, i.e., the fact that the profile has two maxima (104 and 225°C). The first maximum coincides with the beginning of production of the low-temperature N_2/N_2O peaks. The reason for the decreased NO desorption at these temperatures is that the NO can interact with the proposed "bidentate" NO on the surface, and generate N_2 and N_2O. In the case of the second maximum this is due to the fact that the NO molecules (at these higher temperatures) now have sufficient energy to dissociate on the surface and form N_{ads} intermediates which can go on to form N_2 and N_2O.

DISCUSSION

The temperature programmed reaction results (Fig. 1) show that the production of N_2/N_2O occurs in two stages. At low temperature the dissociation of NO is unfavourable; otherwise, the rate of N_2 production would be higher. In fact, N_2O is the most abundant product under these conditions. As the temperature is increased the conversion to N_2O reaches a maximum and then begins to decrease. This can be understood in terms of a competition between an increasing probability for the dissociation of adsorbed NO_{ads}, and the decreasing concentration of adsorbed NO. The predominant reactions at the higher temperatures are the formation of N_2 or NH_3.

The SSITKA results show for all the product molecules (N_2, N_2O, and NH_3) that the trend is for the residence time to decrease as the temperature increases. On the other hand, the concentration of sites that produce N_2 and N_2O increases by a factor of ~4 between 50 and 73°C (see Table 2). Thus, the catalyst produces more N_2O mainly due to an increase in the concentration of sites which are active for this reaction, while the increase in N_2 production arises both because of an increase in the concentration of sites active for N_2 formation *and* an increase in their effective "activity."

Figure 3 shows changes in the fraction of heavy atoms in the product molecules following the switch of ^{14}NO for ^{15}NO. Note that the $\alpha(N_2O)$ profile and the ^{15}NO profile are exactly the same, indicating that the incorporation of a ^{14}N atom into an N_2O molecule does not take place when the gas phase ^{14}NO is fully removed from the system. This is not the case for the formation of N_2 since $^{14}N^{15}N$ is formed for a considerable time after all traces of gaseous ^{14}NO are removed. This may indicate the requirement for gas-phase NO (or adsorbed undissociated NO) in the formation of N_2O. Further mathematical analysis of the properties of the experimental profiles will clarify the nature of the reaction mechanism (36).

The non-steady state isotopic transient kinetic analysis ("stopped-flow") NO switching experiments allow us to examine the nature of the intermediates on the surface. Less of the mixed-labelled N_2O is formed from the switch of ^{15}NO over the catalyst after an interval in H_2 than is formed from the true SSITKA experiment. Therefore, we conclude that the treatment in H_2 results either in the desorption of N_2O precursors or in their conversion into N_2 precursors. We can also say that some spectator species on the surface are converted into N_2 precursors by the H_2 treatments because the decrease in N^*NO formation does not fully account for the increase in N^*N formation.

A preliminary analysis of the SSITKA experiments shows that in the formation of N_2 and N_2O at least one of the surface intermediates is not used in the formation of both products. Also, comparing the SSITKA with the "stopped-flow-switching" experiments we conclude that intermediates leading to N_2O are short lived and not stable on the surface while those leading to N_2 are more stable.

CONCLUSIONS

For the production of N_2O on our Pt catalyst we conclude:

- after a peak production at 100°C, selectivity to N_2O decreases as the temperature of reaction is raised (as determined from the TPR_{xn} experiment);
- the production of N_2O seems to require gas-phase, or weakly adsorbed, NO;
- the rate of N_2O production increases with temperature primarily because the concentration of sites active for this reaction on the catalyst increases; i.e., an increase in the effective activity of the sites is not as important as an increase in the concentrations of sites;
- N_2O is produced isotopically first, so therefore there are surface intermediates which do not go on to form N_2O, i.e., the ^{14}N species that produce N_2;
- some intermediate in the chain for the production of N_2O is not stable under an H_2 atmosphere at 60°C (as determined from the NSSITKA experiments).

For N_2 formation we can conclude:

- N_2 is produced with more selectivity at higher temperatures (from TPR_{xn});

- the rate of production of N_2 increases with temperature as the concentration *and* effective activity of the sites leading to its production both increase;
- N_2 is produced from more longer lived intermediates in the reaction sequence than N_2O; i.e., it is isotopically second (from SSITKA);
- N_2 intermediates are more stable on the surface than N_2O intermediates, and the latter (or NO_{ads} spectator species) can be transformed into the former by a reductive treatment (from the NSSITKA experiments).

ACKNOWLEDGMENTS

We are grateful to the EPSRC for supporting this research through contract GR/K70403. A.A.S. thanks NATO and The Royal Society for providing a fellowship (NATO/96A).

REFERENCES

1. Taylor, K. C., *Catal. Rev. Sci. Eng.* **35**(4), 457 (1993). [and refs. therein]
2. Bosch, H., and Janssen, F., *Catal. Today* **2**, 4 (1988). [and refs. therein]
3. Ansell, G. P., Golunski, S. E., Hayes, J. W., Burch, R., and Millington, P. J., *Stud. Surf. Sci. Catal.* **96**, 577 (1995).
4. Iwamoto, M., and Mizuno, N., *J. Automobile Eng.* **207**, 23 (1993).
5. Burch, R., and Watling, T. C., *Catal. Lett.* **43**(1-2), 19 (1997).
6. Burch, R., and Watling, T. C., *J. Catal.* **169**(45) (1997).
7. Shelef, M., Otto, K., and Gethi, H., *Atmos. Environ.* **3**, 107 (1969).
8. "Ozone in the United Kingdom 1993," third report of the United Kingdom Photochemical Oxidants Review Group, Dept. of the Environment, 1993.
9. d'Itri, J. L., and Schatler, W. M. H., *Appl. Catal. B Environ.* **15**, 298 (1992).
10. Hums, E., *in* "214th ACS National Meeting, Las Vegas Nevada, Sept. 1997," p. 1, 1997.
11. Burch, R., and Scire, S., *Appl. Catal. B Environ.* **3**, 295 (1994).
12. *Catal. Today*, 26 (1995). [R. Burch, Ed.]
13. *Catal. Today*, 22 (1994). [M. Iwamoto, Ed.]
14. Burch, R., and Watling, T. C., *J. Catal.* **169**, 45 (1997).
15. Captain, D. K., Robberts, K. L., and Amaridis, M. D., *Catal. Today* **42**, 93 (1998).
16. Sasaki, M., Hamada, H., Kintaichi, Y., Ito, Y., and Tabata, M., *Catal. Lett.* **15**, 297 (1992).
17. Burch, R., and Ottery, D., *Appl. Catal. B Environ.* **9**, L19 (1996).
18. Burch, R., and Coleman, M., *Appl. Catal. B Environ.*, in press.
19. Armor, J. N., *Appl. Catal. B Environ.* **1**, 221 (1992).
20. Happel, J., *Chem. Eng. Sci.* **33**, 1567 (1978).
21. Bennett, C. O., *in* "Catalysis Under Transient Conditions" (A. T. Bell, and L. L. Hegedus Eds.), ACS Symposium Series, Vol. 178, p. 1. Am. Chem. Soc. Washington, DC, 1982.
22. Biloen, P., *J. Mol. Catal.* **21**, 17 (1982).
23. Hanssen, K. F., Blekkan, E. A., Schanke, D., and Holmen, A., *Stud. Surf. Sci. Catal.* **109**, 193 (1997).
24. Bajusz, I. G., Kwik, D. J., and Goodwin, J. G., *Catal. Letts.* **48**(3-4), 151 (1997).
25. Efstathiou, A. M., and Verykios, X. E., *Appl. Catal. A General* **151**(1), 109 (1997).
26. Ali, S. H., and Goodwin, J. G., *J. Catal.* **170**(2), 265 (1997).
27. Oukaci, R., Blackmond, D. G., Goodwin, J. G., Jr., and Gallagher, G. R., *in* "Catalytic Control of Air Pollution," Ch. 5, pp. 61–72. Am. Chem. Soc., Washington, DC, 1992.
28. Frost, J. C., Lafyatis, D. S., Rajaram, R. R., and Walker, A. P., "4th International Congress on Catalysis and Automotive Pollution Control, Brussels, April 1997," Vol. 1, p. 129, O14, 1997.
29. Efstathiou, A. M., and Fliatoura, K., *Appl. Catal B Environ.* **6**(1), 35 (1995).
30. Janssen, F. J. J. G., Van Den Kerkhof, F. M. G., Bosch, H., and Ross, J. R. H., *J. Phys. Chem.* **91**(27), 6633 (1987).
31. Kumthekar, M. W., and Ozkan, U. S., *J. Catal.* **171**(1), 54 (1997).
32. Burch, R., and Sullivan, J. A., *J. Catal.* **182**(2), 489 (1999).
33. Burch, R., Shestov, A. A., and Sullivan, J. A., *J. Catal.* **182**(2), 497 (1999).
34. "Eight Peak Index of Mass Spectra," 3rd ed. Unwin Brothers, Surrey, 1983.
35. Shannon, S. L., and Goodwin, J. G., *Chem. Rev.* **95**, 677 (1995).
36. Burch, R., Shestov, A. A., and Sullivan, *J. Catal.* **186**, 363 (1999).
37. Hecker, W. C., and Bell, A. T., *J. Catal.* **92**(2), 247 (1985).
38. Burch, R., and Watling, T. C., *Catal. Letts.* **37**, 51 (1996).